THE ROYAL SOCIETY biology letters

Preliminary evaluation of nanoscale biogenic magnetite in Alzheimer's disease brain tissue

D. Hautot[1], Q. A. Pankhurst[1], N. Khan[2] and J. Dobson[3*]

[1]*Department of Physics and Astronomy, University College London, London WC1E 6BT, UK*
[2]*Department of Neuropathology, Institute of Psychiatry, King's College London, De Crespigny Park, London SE5 8AF, UK*
[3]*Department of Biomedical Engineering and Medical Physics, Centre for Science and Technology in Medicine, Keele University, Thornburrow Drive, Hartshill, Stoke-on-Trent ST4 7QB, UK*
[*]*Author for correspondence (jdobson@keele.ac.uk).*

Recd 31.01.03; *Accptd* 26.02.03; *Online* 09.04.03

Elevated iron levels are associated with many types of neurodegenerative disease, such as Alzheimer's, Parkinson's and Huntington's diseases. However, these elevated iron levels do not necessarily correlate with elevated levels of the iron storage or transport proteins, ferritin and transferrin. As such, little is known about the form of this excess iron.

It has recently been proposed that some of the excess iron in neurodegenerative tissue may be in the form of the magnetic iron oxide magnetite (Fe_3O_4). We demonstrate, for the first time to our knowledge, using highly sensitive superconducting quantum interference device (SQUID) magnetometry, that the concentrations of magnetite are found to be significantly higher in three samples of Alzheimer's disease tissue than in three age- and sex-matched controls. These results have implications, not only for disease progression, but also for possible early diagnosis.

Keywords: Alzheimer's disease; iron; magnetite; ferritin

1. INTRODUCTION

Iron is essential for virtually all living organisms. However, some forms of iron are potentially toxic to living cells. In most organisms, including humans, iron is stored in a relatively safe, oxidized state (Fe^{3+}) within ferritin—a hollow spherical protein shell 12 nm in diameter and capable of sequestering up to 4500 iron atoms in the form of ferrihydrite ($5Fe_2O_3{\cdot}9H_2O$), which is mineralized in the protein's core. Iron is transported into the ferritin shell via three- and fourfold channels at the junctions of the protein's subunits. During this process, potentially toxic Fe^{2+} is oxidized for storage as ferrihydrite.

In humans, abnormal accumulations of iron have been shown to be associated with many types of neurodegenerative diseases, such as Alzheimer's disease (AD), Parkinson's disease (PD) and Huntington's disease (HD) (Beard *et al.* 1993; Smith *et al.* 1997). Although this association was first discovered in AD tissue by Goodman in 1954 (Goodman 1953), the increase in iron does not appear to be related to an increase in levels of the ferritin protein or the iron transport protein transferrin (e.g. Beard *et al.* 1993). For this reason, progress in understanding the role of this excess iron and the form in which it occurs has been relatively slow.

It has recently been proposed that some of the excess iron in neurodegenerative tissue may be present in the form of magnetite—a magnetic iron oxide that was discovered in human brain tissue samples in 1992 by J. L. Kirschvink and others (Kirschvink *et al.* 1992; Dobson 2001). Magnetite is a magnetic (ferrimagnetic) iron oxide with alternating lattices of Fe^{2+} and Fe^{3+} ions, which is capable of producing free radicals via the Fenton reaction or via triplet state stabilization (Kirschvink 1992; Scaiano *et al.* 1997; Chignell & Sik 1998). Recent experiments have also demonstrated that iron–oxygen complexes may be even more effective catalysts for free-radical damage in brain tissue than the Fenton reaction (Schafer *et al.* 2000), so the potential deleterious effect of magnetite is possibly even more significant. To examine this theory and determine whether there are disease-related variations in biogenic magnetite content in AD tissue, we performed a detailed analysis and comparison of the magnetic properties of tissue samples from three AD subjects and three age- and sex-matched controls.

2. MATERIAL AND METHODS

Fresh-frozen brain tissue removed during autopsy from three subjects with confirmed AD and three age- and sex-matched control subjects was obtained from the UK Medical Research Council London Neurodegenerative Diseases Brain Bank through an informed donor consent programme (a summary of case details is provided in table 1). All tissue samples were resected using acid-cleaned surgical instruments. The sampled area of known pathology for AD was the superior temporal gyrus (at the level of the lateral geniculate body). This same area was also sampled for the controls. The dissected samples were *ca.* 1 cm^3 in volume and were stored in a deep freeze at 193 K before preparation for measurement of the magnetic properties.

Sample preparation involved freeze-drying the tissue to remove water and concentrate the volume fraction of iron species within the tissue solids. Each sample was then carefully ground to a powder with a clean mortar and pestle, introduced into a plastic sample holder, and pressed into a pellet of diameter 5 mm and height 2–4 mm (an optimal geometry for the SQUID measurements) using a custom-made non-magnetic press.

The magnetic properties of all six tissue samples were measured using a Quantum Design MPMS-7 (SQUID) magnetometer. As SQUID magnetometry is highly sensitive, it is the method of choice to measure very weakly magnetic material. It was used in the present study to examine the concentrations of magnetite in the presence of not only a large diamagnetic signal from the tissue but also ferritin, which has a ferrihydrite core with magnetic properties that differ significantly from magnetite. The detection of magnetite in bulk tissue samples can be difficult because in bulk samples it is generally measured in the presence of ferritin and usually in significantly lower concentrations. To separate the magnetite signal from the diamagnetic and ferritin background, three different but complementary magnetic measurements were performed.

(i) M–H curves: magnetization (M) measured as a function of applied field (H). These 'hysteresis loops' were analysed in accordance with a model of superposition of the M–H characteristics of magnetite, ferritin and diamagnetic tissue to extract the relative concentrations of all signal components.
(ii) IRM curves: isothermal remanent magnetization (IRM). This is a measure of the remanent magnetization acquired in a sample as it is exposed to incrementally increasing applied magnetic fields at a fixed temperature. Measurement of the remanence is made in the absence of an applied field, thus eliminating contributions from diagmagnetic and paramagnetic components within the tissue sample. Measurements were made at 150 K, which excludes any magnetic contributions from ferritin (ferritin is superparamagnetic and behaves as a paramagnet at this temperature), from the diamagnetic bulk tissue and from any paramagnetic ions, and detect only the remanence due to magnetically blocked particles in the tissue.

DOI 10.1098/rsbl.2003.0012

Table 1. Summary of the sample data. 'PM interval', the post-mortem interval between death and autopsy; 'agonal state', the established cause of death; and 'magnetite concentration', units of micrograms of magnetite per gram of freeze-dried tissue. The ratio of dry to wet tissue masses was *ca.* 0.25 in each case. All six subjects were female. Subjects A, B and D had Alzheimer's disease, while subjects D, E and F were controls. The uncertainties quoted reflect the statistical error of the fitting process only.

subject	age (years)	PM interval (h)	agonal state	magnetite concentration ($\mu g\, g^{-1}$)	disease duration (years)
A	86	12	broncho-pneumonia	1.0 ± 0.4	10
B	82	55	hypostatic pneumonia	1.1 ± 0.1	8
C	89	24	broncho-pneumonia	7.0 ± 0.3	3–4
D	76	66	not available	0.4 ± 0.3	—
E	82	32	pneumonia	0	—
F	68	53	ischaemic heart disease	0	—

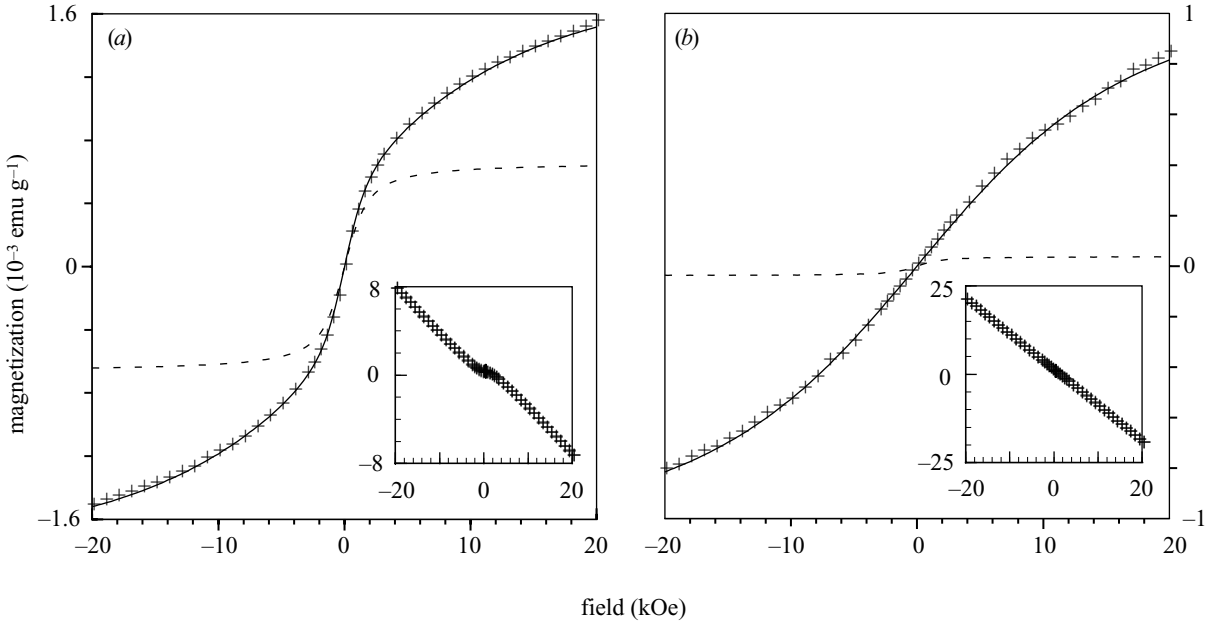

Figure 1. (*a*) Sample magnetization versus applied magnetic field (M–H curve) measured at 150 K for AD sample C showing the averaged part of the magnetization (crosses) remaining after subtraction of the linear components from the raw curve (inset). The solid line through the data points is a fit to a combination of magnetite and ferritin Langevin functions; the dashed line that does not coincide with the data points shows the calculated magnetite component only. (*b*) The same curves as in part (*a*) for control sample D in which the magnetic response is dominated by ferritin and the magnetite component is much smaller.

(iii) M–T measurements: magnetization (M) measured as a function of temperature (T). The measurements are made during warming in an external field and can be obtained under zero-field-cooled (ZFC) or field-cooled (FC) conditions. This is a particularly effective way to identify the mean blocking temperature of a sample.

3. RESULTS

To measure the magnetite content of the samples, magnetization data (M–H hysteresis loops) were recorded and compared at 150 K. This is above the blocking temperature for ferritin so that any hysteresis would be due to other magnetic compounds. The M–H curves show a response that is dominated by a diamagnetic component due to the tissue (linear with a negative slope) plus a small magnetic contribution due to the iron-containing species, which is best seen after subtracting the diamagnetic contribution (figure 1). To account for the presence of both nanoscale (superparamagnetic) magnetite and magnetically blocked magnetite particles, the up and down branches of the M–H curves were averaged (Allia *et al.* 1999) and the resulting anhysteretic curves were fitted as a sum of Langevin functions for ferritin and magnetite (figure 1). A linear function was also included to account for the contribution from the diamagnetic tissue and a smaller contribution from paramagnetic components. The M–H curves for ferritin were constrained to match those of the best available published data for horse spleen ferritin (Makhlouf *et al.* 1997), and the amount of ferritin was the only variable. For magnetite, the saturation magnetization was fixed to 95.3 emu g^{-1} (Anonymous 1970) at 150 K and both its quantity and an effective mean magnetic moment per particle were refined.

The results of SQUID magnetometry measurements conducted on human brain tissue samples were consistent with the presence of ferritin in the samples and, in some cases, magnetite. The temperature dependence of the magnetization under FC and ZFC conditions showed a

mean superparamagnetic blocking transition at *ca.* 8 K—a transition that is characteristic of the nanoscale ferrihydrite core of ferritin (Dubiel *et al.* 1999). Magnetite was identified in some samples through IRM measurements. These data, recorded at 150 K (well above the blocking temperature of ferrihydrite), revealed the presence of a population of magnetically blocked particles that saturated at *ca.* 3 kOe, a field that is characteristic of magnetite (Anonymous 1970).

These analyses show that the samples are divided into two groups: one with a substantial amount of magnetite, and one with very little or no magnetite (table 1). The three samples with substantial amounts of magnetite (between 1 μg and 7 μg of magnetite per gram of dry tissue) were the three AD samples. It is notable that sample C, which had the highest magnetite concentration, came from the individual with the most aggressive and advanced AD at the time of death. Based on available clinical data, this individual had a familial form of AD. This is typified by shorter disease duration and a more severe deposition of pathological lesions, as observed in this case. Further work may help to reveal a correlation between the burden of Alzheimer-type pathology and the biogenic magnetite concentration.

Two out of the three control samples showed no measurable magnetite, and one (sample D) had a low concentration compared with the AD samples ($0.4\ \mu g\ g^{-1}$). Interestingly, sample D showed some pathological changes on autopsy suggestive of a neurodegenerative process (significant plaques and tangles), which had not manifested clinically at the time of the individual's death. It would appear, therefore, that the neurodegenerative condition was at an early pre-clinical stage. The other two controls were both clinically and pathologically normal.

4. DISCUSSION

Although these results are preliminary, they illustrate what appears to be a striking correlation between the amount of nanoscale biogenic magnetite in diseased brain tissue and the onset and progression of Alzheimer's disease. They also demonstrate that magnetite is at least partially responsible for the increase in iron in AD tissue (and, by inference, potentially also in PD and HD tissue), the occurrence of which has been the subject of speculation for almost 50 years.

The presence of anomalous concentrations of magnetite in AD tissue raises interesting questions as to its origin and the role it may have (if any) in the initiation or progression of the disease. As magnetite provides a source of Fe^{2+}, it is possible that its presence results in the enhanced production of free radicals via the Fenton reaction or, as mentioned in § 1, via triplet state stabilization. It is also possible, however, that these accumulations are a by-product of the disease rather than a causative agent.

The results presented here have profound implications for our understanding of the role of iron in neurodegenerative diseases and for the possible early diagnosis of at-risk patients via MRI techniques. Currently, MRI assessment of neurodegeneration is limited to the latter stages of disease progression, when atrophy of the diseased area can be imaged (e.g. Ketonen 1998; Jack *et al.* 1999). The data here suggest that abnormally high concentrations of magnetite may be present in tissue even before clinical manifestation of the condition, thereby providing a method of early detection via the effects of local magnetic fields from the particles on proton relaxation rates in the MRI scanner. Similar techniques are already being employed to quantify iron storage in the liver (Clark & St Pierre 2000) and could potentially be modified to detect anomalous iron concentrations associated with neurodegenerative disorders such as AD.

Acknowledgements

The authors thank Dr Ying Yang (Keele), Dr Simon Carling (Royal Institution), Dr Ellen Platzmann (UCL) and Dr Jane Hutton (Warwick) for help with sample preparation and discussions. This work has been funded by a UK Medical Research Council Discipline Hopping grant.

Allia, P., Coisson, M. K., Knobel, M., Tiberto, P. & Vinai, F. 1999 Magnetic hysteresis based on dipolar interactions in granular magnetic systems. *Phys. Rev.* B **60**, 12 207–12 218.

Anonymous, 1970 *Landolt-Börnstein new series: group III, volume 4b, Magnetic and other properties of oxides and related compounds*. Berlin: Springer.

Beard, J. L., Connor, J. R. & Jones, B. C. 1993 Iron in the brain. *Nutr. Rev.* **51**, 157–170.

Chignell, C. F. & Sik, R. H. 1998 Effect of magnetite particles on photoinduced and non-photoinduced free radical processes in human erythrocytes. *Photochem. Photobiol.* **65**, 598–606.

Clark, P. R. & St. Pierre, T. G. 2000 Quantitative mapping of transverse relaxivity (1/T2) in hepatic iron overload: a single spin-echo imaging methodology. *Magn. Reson. Imaging* **18**, 431–438.

Dobson, J. 2001 Nanoscale biogenic iron oxides and neurodegenerative disease. *FEBS Lett.* **496**, 1–5.

Dubiel, S. M., Zablotna-Rypien, B., Mackey, J. B. & Williams, J. M. 1999 Magnetic properties of human liver and brain ferritin. *Eur. Biophys. J.* **28**, 263–267.

Goodman, L. 1953 Alzheimer's disease—a clinicopathologic analysis of 23 cases with a theory on pathogenesis. *J. Nerv. Ment. Dis.* **118**, 97–130.

Jack, C. R. (and 9 others) 1999 Prediction of AD with MRI-based hippocampal volume in mild cognitive impairment. *Neurology* **52**, 1397–1402.

Ketonen, L. M. 1998 Neuroimaging of the aging brain. *Neurol. Clinics* **16**, 581–598.

Kirschvink, J. L. 1992 Comment on 'constraints on biological effects of weak extremely-low-frequency electromagnetic fields'. *Phys. Rev.* A **46**, 2178–2184.

Kirschvink, J. L., Kobayashi-Kirschvink, A. & Woodford, B. J. 1992 Magnetite biomineralization in the human brain. *Proc. Natl Acad. Sci. USA* **89**, 7683–7687.

Makhlouf, S. A., Parker, F. T. & Berkowitz, A. E. 1997 Magnetic hysteresis anomalies in ferritin. *Phys. Rev.* B **55**, R14 717–R14 720.

Scaiano, J. C., Monahan, S. & Renaud, J. 1997 Dramatic effect of magnetite particles on the dynamics of photogenerated free radicals. *Photochem. Photobiol.* **65**, 759–762.

Schafer, F. Q., Qian, S. Y. & Buettner, G. R. 2000 Iron and free radical oxidations in cell membranes. *Cell. Mol. Biol.* **46**, 657–662.

Smith, M. A., Harris, P. L. R., Sayres, L. M. & Perry, G. 1997 Iron accumulation in Alzheimer disease is a source of redox-generated free radicals. *Proc. Natl Acad. Sci. USA* **94**, 9866–9868.